

# New Combination of EXAFS Spectroscopy and Density Fractionation for the Speciation of Chromium within an Andosol

EMMANUEL DÆLSCH,<sup>\*,†</sup>  
 ISABELLE BASILE-DÆLSCH,<sup>§</sup>  
 JEROME ROSE,<sup>‡</sup> ARMAND MASON,<sup>‡</sup>  
 DANIEL BORSCHNECK,<sup>‡</sup>  
 JEAN-LOUIS HAZEMANN,<sup>⊥</sup>  
 HERVE SAINT MACARY,<sup>†</sup> AND  
 JEAN-YVES BOTTERO<sup>‡</sup>

CIRAD, Environmental Risks of Recycling Research Unit,  
 Station de La Bretagne, BP 20, Saint-Denis Messagerie Cedex  
 9, La Réunion, F-97408 France, IRD-La Réunion UMR 161  
 (LSTUR), BP 172, Sainte-Clotilde Cedex, F- 97492 France,  
 CEREGE UMR 6635 CNRS–Université Paul Cézanne  
 Aix-Marseille III, IFR PMSE 112, Europôle Méditerranéen de  
 l'Arbois, BP 80, Aix-en-Provence Cedex 04, F-13545 France,  
 and Laboratoire de Cristallographie, BP 166,  
 Grenoble Cedex 09, F-38042 France

Studying speciation of heavy metals instead of their total concentration in a complex matrix such as soil is a scientific challenge that requires a combination of different analytical techniques. We compared the speciation of Cr within an andosol (island of Réunion) by using X-ray absorption spectroscopy (XAS) and sequential extraction. Contradictory results were obtained since the fraction of Cr bound to organic matter was detected only with the latter method. As bulk soil is rather complex, its fractionation by a densimetric method decreased its heterogeneity. We found that 60% Cr was within chromite-type primary minerals. Weathering of these phases led to Fe and Cr release, eventually resulting in either coprecipitation as mixed Fe–Cr oxyhydroxide (16% total Cr) or precipitation of a Cr oxyhydroxide (5% total Cr). Our results also revealed that 13% Cr was bound to organic matter. The organic matter was complexed with mineral phases to form organomineral complexes with a density ranging from 1.9 to 2.6. The use of an original density fractionation-based sample preparation allowed identification of the role of organic matter in chromium speciation within an andosol and to overcome the difficulties of EXAFS to detect light elements in the vicinity of heavy elements.

## Introduction

It is essential to study the speciation of heavy metals to accurately determine their mobility, bioavailability, and potential toxicity. Chromium is quite significant in this respect, since its two common oxidation states present in

the environment differ drastically in terms of charge, physicochemical properties, chemical, and biochemical reactivity. Cr<sup>3+</sup> is considered to be an essential trace element for the functioning of living organisms responsible for glucose and lipid metabolism in mammals (1). Conversely, Cr<sup>6+</sup> is an oxidizing agent that can diffuse across cell membranes while inducing toxic reactions in humans (skin allergies, dermal necrosis, bronchogenic carcinoma) (2, 3). Moreover, Cr<sup>6+</sup> compounds are usually highly soluble, mobile, and bioavailable in comparison to barely soluble Cr<sup>3+</sup> species (4).

In non-contaminated soils, Cr is inherited from parent rocks. The Cr released during the weathering of bearing phases (spinel or silicates) can subsequently react with various soil components: Cr can substitute Fe in oxides and oxyhydroxides (5), sorbed on surface of Fe oxides (6), substitute Al in octahedral layer of clays, sorbed on surface of phyllosilicates (7) or can be complexed into stable organomineral complexes (8). These reactions have been mainly examined in batch experiments with pure and synthetic component. Few studies deal with the speciation of Cr within actual soil (9–13) and the analytical techniques used by the authors (X-ray diffraction, sequential extraction, microscopy, etc.) failed to quantify the Cr repartition between the different soil components.

Analysis of heavy metal speciation within a multicomponent system such as soils is still a scientific challenge requiring a combination of several analytical techniques (14). They should enable researchers to differentiate the potential heavy metal-bearing phases (e.g., primary minerals, secondary minerals, organics, etc.) and to describe the different types of interaction between heavy metals and soil components (e.g., sorption, precipitation, etc.). Recent advances in synchrotron-based X-ray absorption spectroscopy (XAS) have led to important innovations and increased our knowledge on trace element speciation (15). Extended X-ray absorption fine structure (EXAFS) spectroscopy is a very powerful technique for describing the local environment of a target atom, but it still needs improvements for use with complex matrices.

First, this spectroscopy provides information about the predominant species, so minor phases can be overlooked without appropriate sample preparation. In recent studies, selective sequential extraction was combined with EXAFS spectroscopy to investigate zinc (16) and arsenic (17) speciation in soils. Nevertheless, problems involving the nonselectivity of reagents or readsorption of elements following release are frequently reported (18).

Also, it is frequently difficult to detect "light" neighboring atoms (such as C) around heavier ones using EXAFS. The role of organic matter in heavy metal sorption could thus be overlooked when considering soils with a complex mixture of heavy metal-bearing phases.

Here we report the speciation of Cr within an andosol. We used a new approach based on physical soil fractionation prior to speciation analyses in order to overcome the cited shortcomings of EXAFS. The objective was to separate the different minerals and organomineral complexes according to their density. These separations were performed to limit the number of Cr-bearing phases for each fraction and to facilitate the study of Cr speciation.

The advantages of this novel method are evaluated by comparing the following:

- chemical sequential extraction and Cr K-edge EXAFS analysis of bulk soil;
- the results of chemical analysis and Cr K-edge EXAFS analysis of the densimetric soil fractions.

\* Corresponding author phone: (262) 262 52 80 30; fax: (262) 262 52 80 21; e-mail: emmanuel.doelsch@cirad.fr.

<sup>†</sup> CIRAD.

<sup>§</sup> IRD-La Réunion.

<sup>‡</sup> CEREGE.

<sup>⊥</sup> Laboratoire de Cristallographie.

## Materials and Methods

### Soil Localization, Sampling Procedure, and Soil Properties.

We studied a silic Andosol from the volcanic island of Réunion (19). The soil was developed from a phreato-magmatic deposit from the Piton de la Fournaise volcano (20). The sampling site was located on the windward coast (21°09' S; 55°46' E; elevation 470 m) under a secondary tropical forest (mean precipitation 3460 mm·yr<sup>-1</sup>; mean temperature 23.2 °C). In a pit, the homogeneous andic horizon was collected within the 22–50 cm depth range and subsampled from 40 to 50 cm depth for the density fractionation experiments.

For major and trace element analyses, the air-dried and 2 mm sieved soil sample was ground to 100 μm before dissolution. The soil was acidic (pH<sub>water</sub> = 4.5) and C<sub>organic</sub> rich (35.9 g·kg<sup>-1</sup>) at 40–50 cm depth. For the same depth, SiO<sub>2</sub>, Fe<sub>2</sub>O<sub>3</sub>, Al<sub>2</sub>O<sub>3</sub>, and Mn were, respectively, 24.9%; 18.9%; 16.6%, and 1325 mg·kg<sup>-1</sup>. The heavy metal concentrations were high, especially Cr (421 mg·kg<sup>-1</sup>) and Ni (523 mg·kg<sup>-1</sup>), which were clearly above world average, i.e., 54 and 22 mg·kg<sup>-1</sup>, respectively (21). These high concentrations have been explained by the geochemical background of the volcanic island of Réunion (22).

**Sequential Extraction Protocol.** The sequential extraction scheme was first proposed by the Geological Survey of Canada (23). Six different fractions were considered: exchangeable (0.1 M NaNO<sub>3</sub>), adsorbed (1 M CH<sub>3</sub>COONa at pH 5 with CH<sub>3</sub>COOH), bound to organic matter (0.1 M Na<sub>4</sub>P<sub>2</sub>O<sub>7</sub>), bound to amorphous oxyhydroxides (0.25 M NH<sub>2</sub>OH·HCl in 0.05 M HCl–60 °C), bound to crystalline oxides (1M NH<sub>2</sub>OH·HCl in 25% CH<sub>3</sub>COOH–90 °C), and bound to the mineral matrix (also called the “residual fraction”, digestion with a mixture of HF, HNO<sub>3</sub> and HClO<sub>4</sub>). The experimental protocol is described in detail elsewhere (24). Reagents were analytical grade and only ultrapure water was used. Glass- and plasticware used for the experiments were soaked overnight in 5% (v/v) nitric acid and rinsed with ultrapure water. Four replicates were performed with two blanks. The trace element concentrations were determined with an inductively coupled plasma optical emission spectrometer (ICP-OES Vista-PRO, Varian Inc.).

**Density Fractionation.** Six 10 g soil samples were placed in 70 mL centrifuge tubes with 50 mL of deionized water. The samples were sonified with a 0.5 in. probe tip sonifier (Vibracell 750 W, Bioblock Scientific) operating at 35% output to disperse the soil aggregates. The supernatant water was sucked off on a centrifuge tube and freeze-dried. The residual sample was successively subjected to sodium polytungstate solutions at *d<sub>i</sub>* densities of 1.9, 2.3, 2.6, and 2.9 g·cm<sup>-3</sup> (hereafter, density thresholds are reported without stating g·cm<sup>-3</sup>). For each *d<sub>i</sub>* density step, the soil sample was redispersed by 3 min sonification at 70% output before centrifugation. The supernatant of each *d<sub>i</sub>* was sucked off and placed in a 1 l Nalgene bottle. The residual sample was subjected to the same density *d<sub>i</sub>* and the sucked off supernatant was added to the Nalgene bottle. This experiment was performed four times for each density *d<sub>i</sub>*. The collected supernatants of a density *d<sub>i</sub>* were then diluted with deionized water to decrease the solution density to below *d<sub>i-1</sub>*. The solution was then centrifuged to collect the soil fraction within the *d<sub>i-1</sub>* < *d* < *d<sub>i</sub>* density range. Each collected fraction was rinsed and sonified in deionized water three times, centrifuged, and freeze-dried. A more complete description of this experiment can be found elsewhere (25).

**X-ray Diffraction.** XRD patterns of the bulk and densimetric soil fractions were recorded with a Philips PW 3710 X-ray diffractometer using CoK $\alpha$  radiation at 40 kV and 40 mA (a counting time of 8 s per 0.02° step was used for the 2 $\theta$  range 3–80).

**X-ray Absorption Spectroscopy (XAS).** Cr K-edge X-ray absorption spectra were recorded at room temperature on

beamline FAME at the European Synchrotron Radiation Facility (Grenoble, France). The spectra were recorded in fluorescence mode using a 30-elements solid-state Ge detector (Canberra) for the least concentrated samples and measured in transmission mode with a diode for Cr-rich samples. The spectra are the sum of two to four scans depending on the Cr concentration. The energy threshold of the reference Cr-metal foil (*E*<sub>0,ref</sub>) was determined from the maximum of the first derivative of the spectrum and the experimental data were linearly calibrated against the differences between *E*<sub>0,ref</sub> and the absorption edge energy for Cr. The EXAFS function  $\chi(E)$ , is defined as  $\chi(E) = (\mu(E) - \mu_0(E)) / \Delta\mu_0(E_0)$ , where  $\mu(E)$  is the measured absorption coefficient,  $\mu_0(E)$  is the absorption of an isolated atom, and  $\Delta\mu_0$  is the measured jump in the absorption  $\mu(E)$  at the threshold energy *E*<sub>0</sub>. Pre-edge background subtraction and normalization is determined by fitting a linear polynomial to the pre-edge region and a quadratic polynomial to the post-edge region. The difference between these two polynomials extrapolated to the edge energy (*E*<sub>0</sub>) is used as the normalization constant ( $\Delta\mu_0(E_0)$ ).  $\mu_0(E)$  is approximated with a spline function and the background subtraction was performed with the Autobk algorithm and Athena software (26).  $\chi(E)$  is converted to  $\chi(k)$  with the wave number of the photoelectron (*k*). Using a library of Cr model compounds, the Cr-bearing components in the samples (bulk soil and densimetric fractions) were speciated by first utilizing a PCA algorithm to determine the minimum number and type of probable components and then quantified from the experimental EXAFS spectra using a least-square linear combination fitting (LCF).

Our library of Cr model compounds consisted in selected minerals and synthetic compounds. The minerals were chromite (FeCr<sub>2</sub>O<sub>4</sub>), fuchsite (KCr<sub>2</sub>(AlSi<sub>3</sub>O<sub>10</sub>)(OH)<sub>2</sub>), stichtite (Mg<sub>6</sub>Cr<sub>2</sub>(CO<sub>3</sub>)(OH)<sub>16</sub>·4H<sub>2</sub>O), uvarovite (Ca<sub>3</sub>Cr<sub>2</sub>(SiO<sub>4</sub>)<sub>3</sub>), eskolaite (Cr<sub>2</sub>O<sub>3</sub>), and smectite (octahedral substitution of Al for Cr). Fe–Cr oxyhydroxide were synthesized by coprecipitation of mixed 1M Fe(NO<sub>3</sub>)<sub>3</sub> and 0.25M Cr(NO<sub>3</sub>)<sub>3</sub> solutions (5). Amorphous hydrous chromic oxide (subsequently called HCO) was obtained by titration of a 1M Cr(NO<sub>3</sub>)<sub>3</sub> solution with NaOH. For both of these syntheses, the precipitates were washed, freeze-dried and ground in an agate mortar. Cr sorbed to poorly crystalline aluminosilicates (subsequently called Cr All/Imo) was prepared by adding 10<sup>-3</sup> M Cr(NO<sub>3</sub>)<sub>3</sub> solution at pH < 3 to 50 mg of a mixture of allophane and imogolite. The equilibrated suspension was centrifuged and freeze-dried, the Cr concentration was 4.5 mM·g<sup>-1</sup> of solid. The poorly crystalline aluminosilicates were synthesized on the basis of cohydrolysis of Al and Si reagents with Al/Si = 2 and OH/Al = 1.8 (27). In order to account for potential Cr-soil organic matter associations, Cr<sub>3</sub>(OH)<sub>2</sub>(OOCCH<sub>3</sub>)<sub>7</sub> was added to the Cr compound library since humics bind Cr predominantly through carboxylic group (28). The EXAFS spectrum of this reference was provided by Professor Yu-Ling Wei of Tunghai University, Taiwan (29).

Principal component analysis (PCA) was applied to  $k\chi(k)$  functions (bulk soil and densimetric fractions) to determine the number of species contained in the samples (30). As the PCA indicator value failed to reach a minimum, the number of primary components was determined by visual examination of the components to detect the distinction between EXAFS-like signal and noise. For the significant components we also verified that their progressive introduction during the spectral reconstruction decreases *R<sub>f</sub>* at least 20%, with  $R_f = \Sigma((\text{data-fit})^2) / \Sigma(\text{data}^2)$ . These criteria enabled to determine three significant components for the studied samples (bulk soil and densimetric fractions). The corresponding species were identified by target transformations which test each individually target (or model compounds) without a priori knowledge on other present species. SPOIL function was

**TABLE 1. Mean Concentration  $\pm$  Standard Deviation and Percentage of Cr ( $n = 4$ ) in the Soil for Each Step of the Sequential Extraction Procedure**

	Cr concentration mg·kg <sup>-1</sup> (dry weight)	Cr distribution %
exchangeable	<d.l. <sup>a</sup>	0.0
adsorbed	4.7 $\pm$ 0.1	1.1
organic matter	72.1 $\pm$ 2.3	17.4
amorphous oxyhydroxides	12.3 $\pm$ 0.5	3.0
crystalline oxides	53.1 $\pm$ 1.7	12.8
residual	272 $\pm$ 9.5	65.7
sum of fractions	414 $\pm$ 8.3	
total content	421	
recovery (%)	98.3	

<sup>a</sup> <d.l.: under the detection limit.

used to evaluate if a given model compound was an acceptable target. According to this criteria, we selected chromite (SPOIL = 1.4), Cr<sub>3</sub>(OH)<sub>2</sub>(OOCCH<sub>3</sub>)<sub>7</sub> (SPOIL = 2.7), HCO (SPOIL = 3) and we also kept Fe–Cr oxyhydroxide with SPOIL = 3.3.

The last step of EXAFS data analysis was performed by direct fitting of  $k\chi(k)$  functions by least-square optimization of linear combination fit of model compounds. LCF was achieved within a  $k$ -range of 2–10 Å<sup>-1</sup>. Fitting was performed using increments of the four selected model compounds spectra, and a fit was retained when  $R_f$  decreases at least of 20% relative to the previous simulation. For different fits, we tested the precision of the LCF by varying the proportions of the used model compounds. For variations lower than 10%, the shape of the fit was little affected and the variations of  $R_f$  was below 20%. Therefore, we estimated the uncertainty of the LCF method at  $\pm$  15%.

## Results and Discussion

**Chromium Speciation in Bulk Soil.** The reagent blanks for sequential extraction showed no detectable contamination (data not shown). The sequential extraction reproducibility was good with a relative standard deviation less than 11% (Table 1). The recovery (i.e., ratio of the sum of different fractions to the total digestion results) was 98.3%. The Cr concentration in the exchangeable fraction was below the detection limit. For the adsorbed fraction, the Cr concentration was very low, viz. 1.1% of the total Cr content. 17.4% Cr was associated with organic matter, which was close to the concentration of Cr associated with amorphous and crystalline oxides (15.8%). The main Cr fraction was represented by the residual fraction at 65.7% of the total Cr content. In soils derived from serpentinite (9, 10, 12), it was argued that most Cr is bound in the structure of primary minerals such as Cr-rich spinels (i.e., chromite) and Cr-substituted Fe oxides. The most common form of Cr in 12 agricultural soils from Turkey (11) was found to be the residual form (mean value 89.8%) followed by the organic form (7.1%). Under temperate climate, the Cr released by the weathering of basaltic rocks was mainly captured by Fe oxyhydroxides and an organomineral matrix (13). This latter was the dominant weathered phase and contained up to 270 mg·kg<sup>-1</sup> of Cr. We also observed a substantial proportion of Cr linked with organic matter (17.4%). This high proportion was in good agreement with the high affinity of Cr for organic matter (21).

The minerals identified by XRD (see diffractogram in the Supporting Information) were iron oxides (hematite, magnetite), aluminum hydroxide (gibbsite), iron-titanium oxide (ilmenite), phyllosilicates (talc, smectite), nesosilicate (olivine), clinopyroxene (augite), feldspar (anorthite), and quartz. The diffractogram of the bulk soil exhibited also diffuse bands

which cannot be attributed to amorphous organic matter or amorphous ferric hydroxide (their presence was tested by appropriate dissolutions prior X-ray analysis with H<sub>2</sub>O<sub>2</sub> and Tamm reagent). These diffuse bands detected at 4.2, 3.3, 2.5, and 2.2 Å may, therefore, correspond to poorly crystalline aluminosilicates (31).

At first it is worth noting that the total concentration of chromium is quite high (421 mg·kg<sup>-1</sup>) concerning the “average” content of Cr in non-contaminated soil, but quite low regarding the sensitivity of synchrotron X-ray beamlines. Moreover, the EXAFS spectrum of the bulk soil (as well as densimetric fractions) was disturbed by the presence of two edges: L<sub>β</sub> of Ce and L<sub>α</sub> of Nd (see asterisks in Figure 1). The fluorescence detector resolution (200 eV) was not sufficient to separate the fluorescence lines of Cr (5410 eV) with Ce and Nd (around 5200 eV). Nevertheless, the signal/noise ratio is high enough to interpret the data. Comparison of the EXAFS spectra (Figure 1) revealed some similarities between the soil samples and the references. In the bulk soil samples, we detected a shoulder at 5 Å<sup>-1</sup> and an oscillation at 8.7 Å<sup>-1</sup>, similar to the case of chromite and Fe–Cr oxyhydroxide, respectively (see arrows and gray-shaded circles in Figure 1). The LCF results for the bulk soils (Figure 2) showed close agreement between experimental and fitted data, with the contributions of 33% HCO, 40% chromite and 29% Fe–Cr oxyhydroxide. These results are consistent with the bulk soil mineralogical composition, i.e., olivine and Fe oxides detected by XRD. Olivine crystals derived from basaltic lavas from the Piton de La Fournaise volcano are characterized by the presence of chromite inclusions (32), i.e., 40% Cr occurs in the soil as a primary mineral phase. The remaining Cr is associated with secondary mineral phases such as HCO and mixed Fe–Cr oxyhydroxides.

The Cr speciation derived from EXAFS and from sequential chemical extraction were poorly correlated. The chemical extraction revealed that 15.8% of Cr was found in amorphous/crystalline oxide fraction and 65.7% in residual fraction. These two fractions (81.5% of Cr) should correspond to chromite, HCO and Fe–Cr oxyhydroxides according to the LCF of the EXAFS spectrum. Nevertheless, the second largest Cr pool determined by chemical extraction was the organic matter fraction (17.4%). This contribution was not detected in the EXAFS spectrum of the bulk soil. At this point, the contradiction between the sequential extraction results (significant Cr fraction bound to soil organic matter) and the EXAFS results (Cr entirely bound to inorganic phases) could not be overcome due to the difficulty in detecting carbon neighbors by EXAFS.

**Chromium Speciation in Densimetric Fractions.** Density fractionation of bulk soil led to the recovery of 95.4% of the initial soil mass (Table 2). The distribution between the different fractions was unequal, ranging from 0.5% of the soil mass for the 1 <  $d$  < 1.9 fraction to 56.9% of the soil mass for the 2.3 <  $d$  < 2.6 fraction. Cr concentrations were measured in five fractions (except for the 1 <  $d$  < 1.9 fraction for which the collected mass was too low). The 82.7% Cr recovery was not as high as with the sequential extraction procedure (98.3%). The Cr concentration of the  $d$  < 1 fraction was very low (1.6 mg·kg<sup>-1</sup>, Table 2), and low for the 1.9 <  $d$  < 2.3 (19.2 mg·kg<sup>-1</sup>) and 2.6 <  $d$  < 2.9 (29.9 mg·kg<sup>-1</sup>) fractions. In contrast, two fractions were characterized by high Cr concentrations, i.e., 2.3 <  $d$  < 2.6 and  $d$  > 2.9, with 136.9 mg·kg<sup>-1</sup> and 160.4 mg·kg<sup>-1</sup>, respectively. These fractions contained 39.3 and 46.1% of the Cr content whereas the 1.9 <  $d$  < 2.3 and 2.6 <  $d$  < 2.9 fractions represented only 5.5 and 8.6% of the total Cr (Figure 3). The C contents of the fractions were also determined and the results are reported in Table 2. The main organomineral fraction was the 2.3 <  $d$  < 2.6 fraction, with 71.4% of the total C. For the 1.9 <  $d$  < 2.3 and 2.6 <  $d$  < 2.9 fractions, the C content was low (11.7

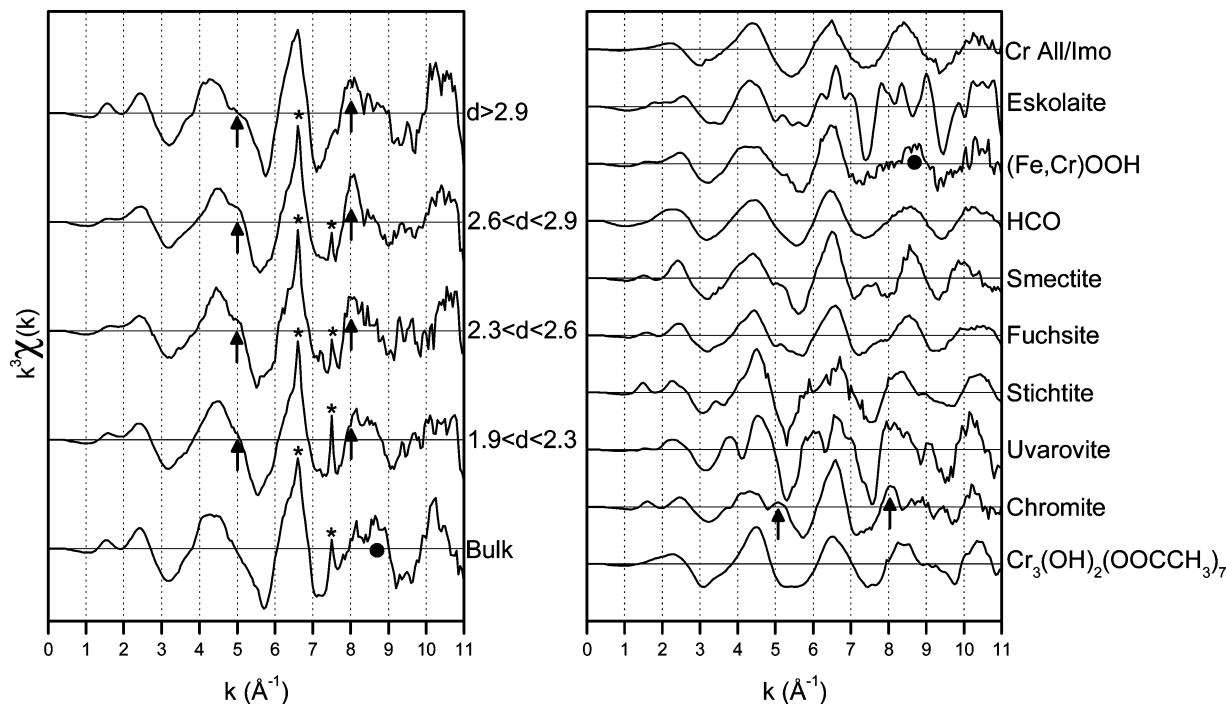


FIGURE 1. Cr K-edge EXAFS spectra for bulk soil and densimetric soil fractions and model compounds used for LCF.

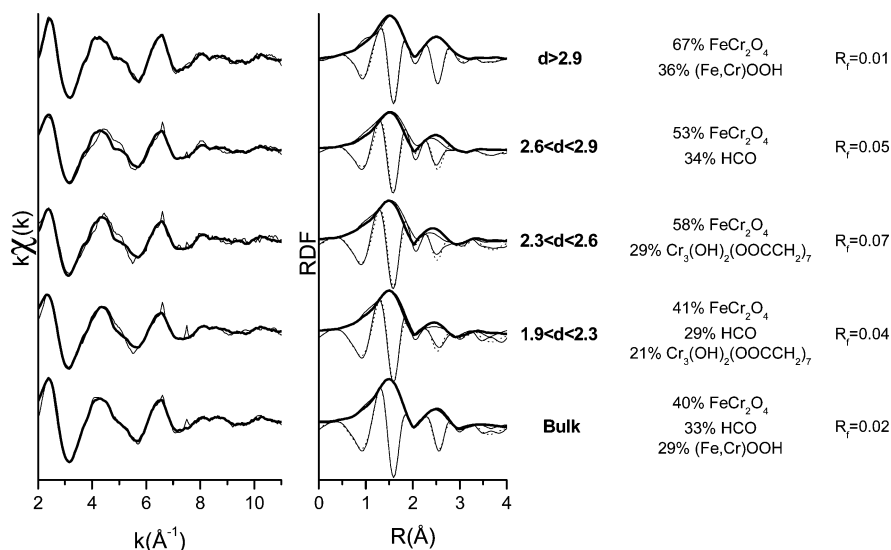


FIGURE 2. Linear fits for the bulk soil and densimetric soil fractions (black line: experimental data and bold line or dashed line: linear combination fit), quantitative compositional results and  $R_f$  corresponding to the quality of the fit with  $R_f = \Sigma((\text{data-fit})^2)/\Sigma(\text{data}^2)$ .

and 8.2%, respectively). Only 1.4% C was measured for the  $d > 2.9$  fraction. Due to the high variability in Cr content in the density fractions, the X-ray patterns of these fractions were recorded to identify potential inorganic Cr-binding minerals.

The diffractograms of the  $1.9 < d < 2.3$ ,  $2.3 < d < 2.6$  and  $2.6 < d < 2.9$  fractions exhibited two contributions: sharp peaks which reflected the high degree of crystallinity of the minerals as well as diffuse bands (see dotted lines in Figure 3) which corresponded to amorphous constituents. For the  $1.9 < d < 2.3$  fractions, X-ray diffraction allowed us to detect the presence of smectite (peaks at 15.4, 4.5, and 3.07 Å, detection confirmed by a glycol test), gibbsite (peaks at 4.8, 4.37, and doublet peak at 3.2 Å) and zeolites (possibly barrerite, peaks at 9.1, 4.05, and 3.02 Å). The mineralogy of the  $2.3 < d < 2.6$  fraction consisted of gibbsite, quartz (peaks at 4.2 and 3.34 Å), smectite and talc (peaks at 9.35, 4.6, and 3.1 Å). The diffractogram of the  $2.6 < d < 2.9$  fraction exhibited

peaks which correspond to feldspar (peaks at 4.03, 3.65, and doublet at 3.24 et 3.21 Å), quartz, smectite, gibbsite, and talc. The diffuse bands detected at 4.2, 3.3, 2.5, and 2.2 Å can be assigned to imogolite or allophane, short-range ordered aluminosilicates, as the exact position and intensity of such bands vary from one study to another (33, 34). Only sharp peaks were present in the X-ray pattern of the  $d > 2.9$  fraction. Iron oxides (hematite, magnetite and/or maghemite, main peak at 2.5 Å), iron oxyhydroxide (goethite, peak at 4.1 Å), clinopyroxene (augite, peak at 2.99 Å), olivine (forsterite, peaks at 3.8 and 2.45 Å), and amphibole (peak at 8.4, 3.1, and 2.7 Å) were detected. Density fractionation of the mineral and organomineral constituents was effective. For instance, minerals detected in this fraction were all have a density of over 2.9:  $d_{\text{magnetite}} = 5.2$ ,  $d_{\text{hematite}} = 5.2$ ,  $d_{\text{goethite}} = 4.26$ ,  $d_{\text{augite}} = 3.51$ ,  $d_{\text{forsterite}} = 3.22$ ,  $d_{\text{actinolite}} = 3.04$ ,  $d_{\text{chlinochlore}} = 2.98 \text{ kg}\cdot\text{dm}^{-3}$ . Only minerals whose densities were close to the cutoff values were simultaneously detected in the fractions

**TABLE 2. Soil Mass, Concentration, and Percentage of Cr and C Associated with the Different Densimetric Fractions**

	soil mass g ( <i>d w</i> )	Cr <sup>a</sup> mg·kg <sup>-1</sup> ( <i>d w</i> )	Cr %	C <sup>a</sup> g·100 g <sup>-1</sup> ( <i>d w</i> )	C %
<i>d</i> < 1	0.10	1.6	0.5	0.23	7.4
1 < <i>d</i> < 1.9	0.07				
1.9 < <i>d</i> < 2.3	1.16	19.2	5.5	0.37	11.7
2.3 < <i>d</i> < 2.6	7.30	136.9	39.3	2.25	71.4
2.6 < <i>d</i> < 2.9	1.30	29.9	8.6	0.26	8.2
<i>d</i> > 2.9	2.90	160.4	46.1	0.04	1.4
sum of fractions	12.83	347.6		3.15	
bulk	13.45	421.0		3.59	
recovery (%)	95.4	82.7		87.7	

<sup>a</sup> Concentration corrected by the sum of the mass fractions, mg·kg<sup>-1</sup> dry weight.

above and below a given cutoff (quartz, with a density of 2.65, was detected in the 2.6 < *d* < 2.9 fractions as well as in the 2.3 < *d* < 2.6 fraction).

There were thus two main densimetric fractions for Cr content, i.e., the 2.3 < *d* < 2.6 and *d* > 2.9 fractions, with 39.3

and 46.1% Cr, respectively. These fractions were characterized by contrasting mineralogy and C content. Indeed, for the 2.3 < *d* < 2.6 fraction, the mineralogy consisted in short-range order aluminosilicate and phyllosilicate, along with 71.4% C, whereas the mineral constituents of the *d* > 2.9 fraction were iron oxides and primary minerals, with a very low C content (1.4%).

XANES spectra were used to infer a Cr oxidation state in the soil samples. The lack of a pre-edge feature in the Cr XANES spectra of the samples demonstrated that chromium was present in the soil as Cr<sup>3+</sup> (35), which is less mobile and toxic than the Cr<sup>6+</sup> form (see spectra in the Supporting Information).

According to the LCF results (Figure 2), Cr speciation of the *d* > 2.9 fraction was dominated by chromite (67%), with a secondary contribution of Fe–Cr oxyhydroxide (36%). For the 2.6 < *d* < 2.9 fraction, the EXAFS spectrum showed the presence of 53% chromite and 34% HCO. The 2.3 < *d* < 2.6 fraction results indicated 58% chromite and 29% Cr<sub>3</sub>(OH)<sub>2</sub>-(OOCCH<sub>2</sub>)<sub>7</sub>. Finally, for the 1.9 < *d* < 2.3 fraction, three compounds were considered in order to enhance the quality of the fit: 41% chromite + 29% HCO + 21% Cr<sub>3</sub>(OH)<sub>2</sub>-(OOCCH<sub>2</sub>)<sub>7</sub>.

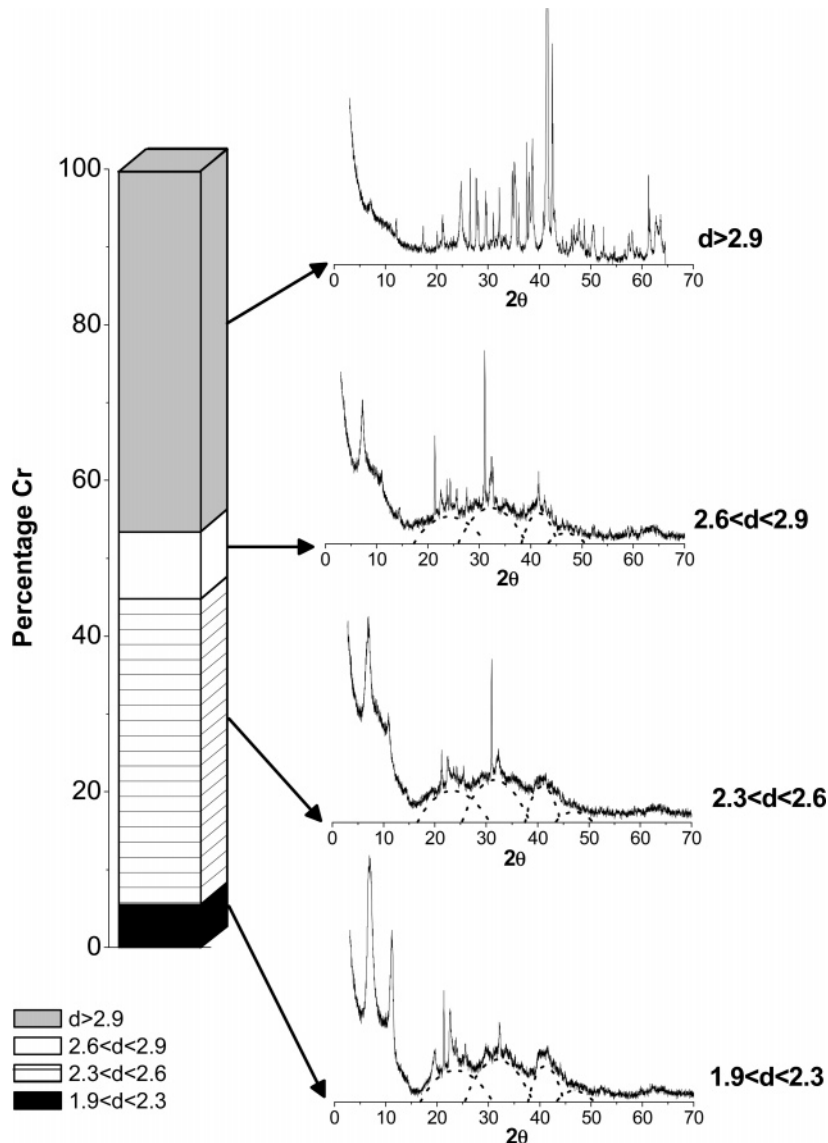


**FIGURE 3. Cr distribution (%) and XRD patterns of the densimetric fractions (dotted line: poorly crystalline aluminosilicates).**

The Cr k-edge EXAFS and XRD results were consistent for the  $d > 2.9$  fraction since the Cr-bearing minerals identified were chromite and Fe–Cr oxyhydroxide. For the other fractions, 40–57.7% of the Cr was present as chromite and HCO was found in the  $2.6 < d < 2.9$  and the  $1.9 < d < 2.3$  fractions. These reference compounds (chromite, HCO and Fe–Cr oxyhydroxide) were also detected in the bulk soil. During natural weathering processes of the parent soil material, especially chromite primary mineral, Fe and Cr are released and transformed into oxides by precipitation. Two main processes have been described to explain the fate of Cr and Fe during this transformation of synthetic samples (6): the adsorption of Cr onto Fe oxides via the formation of inner-sphere surface complexes, where Cr atoms first form surface hydroxyl polymers and then act as nuclei for the precipitation of a surface hydrous Cr oxide; and Cr and Fe coprecipitation, resulting in a mixture of Fe–Cr oxyhydroxide. Therefore, differences in local structure depend on the history of the sample, i.e., coprecipitation of the metal cations versus cation sorption onto a pre-existing oxide. According to the LCF results for the four densimetric fractions, 60% Cr had a local structure close to chromite, 16% Fe–Cr oxyhydroxide and 5% HCO, representing a total of 81%. This sum is comparable to the bulk soil chemical extraction results, i.e., 81.5% corresponding to a sum of 65.7% Cr in the residual fraction and 15.8% associated with amorphous and crystalline oxides.

The main difference between the LCF results for the bulk and densimetric fractions is the use of an organic reference to fit the  $2.3 < d < 2.6$  and the  $1.9 < d < 2.3$  fractions. This was a valid reference since it (i) significantly increased the quality of the fit; and (ii) corresponded to the fractions with the highest C content. Indeed, 11.7 and 71.4% of the organic C was found, respectively, in the  $1.9 < d < 2.3$  and  $2.3 < d < 2.6$  fractions (Table 2). The high C content in the  $1.9 < d < 2.3$  and  $2.3 < d < 2.6$  fractions can be explained by the presence of short-range order aluminosilicates identified by XRD (Figure 3). Indeed, recent results obtained for volcanic ash soil in Réunion clearly demonstrated that poorly crystalline minerals (i.e., allophane and/or imogolite) play an important role in organic C storage (31). Organomineral binding between aluminosilicates and organic C was clearly identified and explained the high residence time of organic C. We thus assume that the Cr fraction linked to organic C correspond to the formation of a complex, i.e., allophane/imogolite-organic C–Cr. To validate the presence of this organomineral association, we also compared these results with the sequential chemical extraction data. Indeed, for the organic Cr fraction, the chemical extractions and LCF results for densimetric fractions were consistent with 17.4 and 13% of the total Cr, respectively.

The chromium speciation in densimetric fractions results confirmed and extended the chromium speciation in bulk soil results. Indeed, we showed that 60% Cr was still bound within chromite-type primary minerals. Weathering of these phases led to Fe and Cr release, eventually resulting in either coprecipitation as mixed Fe,Cr oxyhydroxide (16% total Cr) or precipitation of a Cr oxyhydroxide (5% total Cr). We also determined that 13% Cr was bound to organic matter. This organic matter was complexed with mineral phases to form organomineral complexes having a density ranging from 1.9 to 2.6. We have suggested that the short-range order aluminosilicates identified by XRD could be the mineral phases involved in the organomineral complexes since these poorly crystalline minerals play an important role in organic matter storage. These results are consistent with a poor Cr mobility since the exchangeable and adsorbed forms corresponded only to 1.1% and the chromium was present in the soil as the barely soluble  $\text{Cr}^{3+}$  species.

The Cr concentration within the studied andosol ( $421 \text{ mg}\cdot\text{kg}^{-1}$ ) was above the threshold value ( $150 \text{ mg}\cdot\text{kg}^{-1}$ ) beyond which sewage sludge spreading is unauthorized by French legislation. Recent study of the impact of sewage sludge on heavy metal speciation (24) indicated that this agricultural practice would have no effect on the mobility of Cr. The results of the present study confirm these observations by identifying the Cr-bearing mineral phases. Therefore, sewage sludge spreading could be considered since the law stipulates that a waiver can be issued if it has been proven that this practice would have no impact on the mobility of heavy metals.

The use of an original density fractionation based sample preparation allowed identification of the role of organic matter in chromium speciation within an andosol. This sample preparation procedure enabled to overcome the difficulties of EXAFS to detect of light elements in the vicinity of a heavy element heavy ones. Therefore, this sample preparation procedure could be applied to other complex matrices for heavy metal speciation analyses.

### Acknowledgments

We thank the European Synchrotron Radiation Facility (ESRF) in Grenoble for providing the beamtimes and the FAME team for their helpful and kind assistance during the EXAFS measurements. This work was financially supported by ADEME under project no. 0475C0013 and the European Community (FEOGA), the French Region Réunion, and the Département de La Réunion.

### Supporting Information Available

Figure S1 shows the diffractogram of the bulk soil. Figure S2 presents Cr K-edge XANES spectra for bulk and densimetric fractions of the soil and  $\text{Na}_2\text{CrO}_4$  reference. This material is available free of charge via the Internet at <http://pubs.acs.org>.

### Literature Cited

- Anderson, R. A. Essentiality of chromium in humans. *Sci. Tot. Environ.* **1989**, *86* (1/2), 75–81.
- Shanker, A. K.; Cervantes, C.; Loza-Tavera, H.; Avudainayagam, S. Chromium toxicity in plants. *Environ. Int.* **2005**, *31* (5), 739–753.
- Kotas, J.; Stasicka, Z. Chromium occurrence in the environment and methods of its speciation. *Environ. Pollut.* **2000**, *107* (3), 263–283.
- Fendorf, S. E. Surface reactions of chromium in soils and waters. *Geoderma* **1995**, *67* (1–2), 55–71.
- Schwertmann, U.; Gasser, U.; Sticher, H. Chromium-for-iron substitution in synthetic goethites. *Geochim. Cosmochim. Acta* **1989**, *53* (6), 1293–1297.
- Charlet, L.; Manceau, A. A. X-ray absorption spectroscopic study of the sorption of Cr(III) at the oxide-water interface : II. Adsorption, coprecipitation, and surface precipitation on hydrous ferric oxide. *J. Colloid Interface Sci.* **1992**, *148* (2), 443–458.
- Brigatti, M. F.; Franchini, G.; Lugli, C.; Medici, L.; Poppi, L.; Turci, E. Interaction between aqueous chromium solutions and layer silicates. *Appl. Geochem.* **2000**, *15* (9), 1307–1316.
- Kaupenjohann, M.; Wilcke, W. Heavy metal release from a serpentine soil using a pH-stat technique. *Soil Sci. Soc. Am. J.* **1995**, *59*, 1027–1031.
- Becquer, T.; Quantin, C.; Sicot, M.; Boudot, J. Chromium availability in ultramafic soils from New Caledonia. *Sci. Tot. Environ.* **2003**, *301*, 251–261.
- Gasser, U.; Juchler, S.; Hobson, W.; Sticher, H. The fate of chromium and nickel in subalpine soils derived from serpentinite. *Can. J. Soil Sci.* **1995**, 187–195.
- Koleli, N. Speciation of chromium in 12 agricultural soils from Turkey. *Chemosphere* **2004**, *57* (10), 1473–1478.
- Oze, C.; Fendorf, S.; Bird, D. K.; Coleman, R. G. Chromium geochemistry in serpentinitized ultramafic rocks and serpentine soils from the franciscan complex of California. *Am. J. Sci.* **2004**, *304*, 67–101.
- Soubrand-Colin, M.; Bril, H.; Néel, C.; Courtin-Nomade, A.; Martin, F. Weathering of basaltic rocks from the French Massif

- Central: origin and fate of Ni, Cr, Zn and Cu. *Can. Mineral* **2005**, *43* (3), 1077–1091.
- (14) Morin, G.; Juillot, F.; Ildefonse, P.; Calas, G.; Sanama, J.-C.; Chevallier, P.; Brown, G. E. Mineralogy of lead in a soil developed on a Pb-mineralized sandstone (Largentière, France). *Am. Mineral* **2001**, *86*, 92–104.
- (15) Manceau, A.; Marcus, M. A.; Tamura, N. Quantitative speciation of heavy metals in soils and sediments by synchrotron X-ray techniques. In *Applications of Synchrotron Radiation in Low-Temperature Geochemistry and Environmental Science*; P. Fenter, P., Sturchio, N. C., Eds.; Mineralogical Society of America: Washington, DC, 2002.
- (16) Scheinost, A. C.; Kretzschmar, R.; Pfister, S. Combining selective sequential extractions, X-ray absorption spectroscopy, and principal component analysis for quantitative zinc speciation in soil. *Environ. Sci. Technol.* **2002**, *36* (23), 5021–5028.
- (17) Cances, B.; Juillot, F.; Morin, G.; Laperche, V.; Alvarez, L.; Proux, O.; Hazemann, J.-L.; Brown, G. E.; Calas, G. XAS evidence of As(V) association with iron oxyhydroxides in a contaminated soil at a former arsenical pesticide processing plant. *Environ. Sci. Technol.* **2005**, *39* (24), 9398–9405.
- (18) Martin, J. M.; Nirel, P.; Thomas, A. J. Sequential extraction techniques: Promises and problems. *Mar. Chem.* **1987**, *22* (2–4), 313–341.
- (19) FAO. *World Reference Base for Soil Resources*; Food and Agriculture Organization of the United Nations: Rome, 1998.
- (20) Abchir, A. M.; Semet, M. P.; Boudon, G.; Ildefonse, P.; Bachèlery, P.; Clocchiatti, R. Huge hydrothermal explosive activity on Piton de la Fournaise, Reunion Island: The Bellecombe Ash Member, 2700 BC. In *The European Laboratory Volcanoes, Proceedings of the 2nd workshop*; Casale, R., Fytikas, M., Sigvaldasson, G., Vougioukalakis, G., Eds.; European Commission: Santorini, Greece, 1998.
- (21) Kabata-Pendias, A.; Pendias, H. *Trace Elements in Soils and Plants*, 3rd ed.; CRC Press: Boca Raton, FL, 2001.
- (22) Doelsch, E.; Van de Kerchove, V.; Saint Macary, H. Heavy metal content in soils of Reunion (Indian Ocean). *Geoderma* **2006**, *134* (1–2), 119–134.
- (23) Hall, G. E. M.; Gauthier, G.; Pelchat, J.-C.; Pelchat, P.; Vaive, J. E. Application of a sequential extraction scheme to ten geological certified reference materials for the determination of 20 elements. *J. Anal. Atom. Spectrom.* **1996**, *11*, 787–796.
- (24) Doelsch, E.; Deroche, B.; Van de Kerchove, V. Impact of sewage sludge spreading on heavy metal speciation in tropical soils (Reunion, Indian Ocean). *Chemosphere* **2006**, *65* (2), 286–293.
- (25) Basile-Doelsch, I.; Amundson, R.; Stone, W. E. E.; Borschneck, D.; Bottero, J. Y.; Moustier, S.; Masin, F.; Colin, F. Mineral control of carbon pools in a soil horizon. *Geoderma*, in press.
- (26) Ravel, B.; Newville, M. ATHENA, ARTEMIS, HEPHAESTUS: data analysis for X-ray absorption spectroscopy using IFEFFIT. *J. Synchrotron Rad.* **2005**, *12* (4), 537–541.
- (27) Denaix, L.; Lamy, I.; Bottero, J. Y. Structure and affinity towards Cd<sup>2+</sup>, Cu<sup>2+</sup>, Pb<sup>2+</sup> of synthetic colloidal amorphous aluminosilicates and their precursors. *Colloids Surf., A* **1999**, *158* (3), 315–325.
- (28) Fukushima, M.; Nakayasu, K.; Tanaka, S.; Nakamura, H. Chromium(III) binding abilities of humic acids. *Anal. Chim. Acta* **1995**, *317* (1–3), 195–206.
- (29) Wei, Y.-L.; Lee, Y.-C.; Hsieh, H.-F. XANES study of Cr sorbed by a kitchen waste compost from water. *Chemosphere* **2005**, *61* (7), 1051–1060.
- (30) Ressler, T.; Wong, J.; Roos, J. W.; Smith, L. I. Quantitative speciation of Mn-bearing particulates emitted from autos burning (methylcyclopentadienyl)manganese tricarbonyl-added gasolines using XANES spectroscopy. *Environ. Sci. Technol.* **2000**, *34* (6), 950–958.
- (31) Basile-Doelsch, I.; Amundson, R.; Stone, W.; Masiello, C.; Bottero, J. Y.; Colin, F.; Masin, F.; Borschneck, D.; Meunier, J. D. Mineral control of soil organic carbon dynamic in an allophanic soil (La Réunion). *Eur. J. Soil Sci.* **2005**, *56* (6), 689–703.
- (32) Albarède, F.; Luais, B.; Fitton, G.; Semet, M.; Kaminski, E.; Upton, B. G. J.; Bachèlery, P.; Cheminée, J.-L. The geochemical regimes of Piton de la Fournaise volcano (Réunion) during the last 530 000 years. *J. Petrol.* **1997**, *38* (2), 171–201.
- (33) Parfitt, R. L. Allophane in New Zealand - A Review. *Aust. J. Soil Res.* **1990**, *28*, 343–360.
- (34) Sumner, M. E. *Handbook of Soil Science*; CRC Press: Boca Raton, FL, 2000.
- (35) Shaffer, R. E.; Cross, J. O.; Rose-Pehrsson, S. L.; Elam, W. T. Speciation of chromium in simulated soil samples using X-ray absorption spectroscopy and multivariate calibration. *Anal. Chim. Acta* **2001**, *442* (2), 295–304.

Received for review April 14, 2006. Revised manuscript received October 2, 2006. Accepted October 5, 2006.

ES060906Q